

1
2 **ÖvSim: a Simulation of the Population Dynamics of Mammalian Ovarian**
3 **Follicles**

4
5 Joshua Johnson^{1*}, Xin Chen^{2,3}, Xiao Xu², John W. Emerson⁴

6 **1 University of Colorado Denver, Department of Obstetrics and Gynecology, Division of**
7 **Reproductive Sciences, Building RC2, Room P15 3103, Mail Stop 8613, Aurora, Colorado**
8 **80045, USA**

9 **2 Yale School of Medicine, Department of Obstetrics, Gynecology, & Reproductive**
10 **Sciences, 333 Cedar Street, Tompkins 2-203, New Haven, CT, 06520-8063, USA**

11 **3 Center of Reproductive Medicine, Department of Gynecology and Obstetrics, Nanfang**
12 **Hospital, Southern Medical University, Guangzhou 510515, China**

13 **4 Department of Statistics, Yale University, 24 Hillhouse Avenue, Room B06, New Haven,**
14 **CT, 06520, USA**

15 *** joshua.2.johnson@ucdenver.edu**

16 **Abstract**

17 No two ovaries are alike, and indeed, the same ovary can change its architecture from day to day. This is
18 because ovarian follicles are present in different numbers, positions, and states of maturation throughout
19 reproductive life. All possible developmental states of follicles can be represented at any time, along
20 with follicles that have committed to death (termed follicle atresia). Static histological and whole-mount
21 imaging approaches allow snapshots of what is occurring within ovaries, but our views of dynamic follicle
22 growth and death have been limited to these tools. We present a simple Markov chain model of the
23 complex mouse ovary, called “ÖvSim”. In the model, follicles can exist in one of three Markov states
24 with stationary probabilities, Hold (growth arrest), Grow, and Die. The probability that individual
25 primordial follicles can growth activate daily, the fraction of granulosa cells that survive as follicles grow,

26 and the probability that individual follicles can commit to atresia daily are user definable parameters.
27 When the probability of daily growth activation is stationary at 0.005, the probability of atresia for all
28 follicles is near 0.1, and the probability of granulosa cell survival is modeled around 0.88, $\bar{O}vSim$ simulates
29 the growth and fate of each of the approximately 3000 postpubertal mouse ovarian follicles in a fashion
30 that approximates actual biological measurements (e.g., follicle counts). $\bar{O}vSim$ thus offers a starting
31 platform to simulate mammalian ovaries and to explore factors that might impact follicle development
32 and global organ function.

33 **Author Summary**

34 $\bar{O}vSim$ is a computer simulation of the dynamic growth of mouse ovarian follicles. The program is offered
35 as the beginning of a research and teaching platform to model asynchronous follicle growth and survival
36 or death.

37 **Introduction**

38 A central goal in reproductive biology and medicine is determining mechanisms that control the fates
39 of mammalian ovarian follicles. This is because follicle growth and survival control the availability of
40 the mature eggs used for conception. Follicles also produce endocrine hormones that are key not only
41 for reproduction, but that support health and quality of life. An ovarian follicle consists of a single
42 oocyte and associated somatic cells. After a period of growth arrest in a ‘primordial’ follicle state,
43 growth activation can occur *via* upregulation of mTOR/Akt signaling (1; 2; 3; 4; 5). Somatic granulosa
44 cells begin to proliferate around the oocyte, which itself grows in size and later resumes and completes
45 meiosis (6; 7). Few follicles survive to the final ovulatory stage where they can release a mature egg; the
46 majority of follicles die within the ovary in a process called atresia (8; 9; 10). Because follicles are present
47 in the thousands in reproductive-age mice and humans, and their growth, development and death occur
48 in an asynchronous, stochastic fashion, it can be difficult to conceptualize the ovary’s function(s) as an
49 endocrine organ and how it achieves its consistent production of mature eggs.

50 The most common approaches used to account for the developmental states and survival (or death)
51 of mammalian follicles over time is the preparation of static histological sections of ovaries. These are

52 referred to as histomorphometric approaches (8; 11; 12). Histological sections allow a very detailed
53 micron-scale appreciation for all of the cell types and structures in and around follicles. More recently,
54 whole-mount fluorescence analysis has been used to great effect, providing a finely-grained accounting of
55 the numbers and sizes of follicle-enclosed oocytes in the mouse ovary (13; 14). Future modifications of this
56 latter approach may eventually allow for computer-assisted analysis of the disposition of the somatic cells
57 of follicles as well. The primary drawback of static histomorphometric approaches is the need to prepare
58 specimens from many replicate animals at different time points if differences in follicle composition over
59 time are to be appreciated. Experience with this highly laborious process led us to question whether an
60 *in silico* approach of simulation and analysis of follicle numbers over time was possible.

61 Computer simulations of cells, tissues, and organs are becoming more commonplace. With regards
62 to the ovary, Skodras and Marcelli (15) have produced an interesting graphical and numerical simulation
63 of the size distribution of ovarian follicles in newborn mouse ovaries. Beyond striking graphical images,
64 their study allows the comparison of follicle number in actual (biological) newborn ovaries with realistic
65 simulated counterpart ovaries. As those authors say, such simulations can also support the "...[analysis
66 of the ovary and other] organs made up of large numbers of individual functional units." However, tools
67 for the simulation and visualization of dynamic follicle development within the mammalian ovary over
68 the entire reproductive lifespan have not been available. We hypothesized that establishing a simple set
69 of rules for i) follicle growth activation, ii) granulosa cell proliferation, iii) granulosa cell death, and iv)
70 individual follicle survival could provide the necessary starting points for a rudimentary simulation of
71 stochastic follicle behavior over time. Consideration of these rules led us to a Markov chain approach

72 We reasoned that follicles can exist as growth arrested primordial follicles (a "Hold" state), growing
73 follicles (a "Grow" state), and follicles that have committed to die *via* atresia (a "Die" state). Markov
74 state transition models have been applied as powerful tools in the health and medical literature (e.g., in
75 disease models) (16; 17; 18; 19; 20), and initial modeling of follicles in this way proved fruitful.

76 We have now produced a function in the R language (21), $\bar{O}vSim$, to model follicle Markov state
77 transitions across a discrete time series. $\bar{O}vSim$ simulates follicle development and population dynamics
78 according to user-specified starting population of follicles and transition probabilities. To our surprise,
79 the simple probability model, with informally selected and reasonable parameter values, can produce
80 remarkably accurate representations of follicle population dynamics, closely matching the biologically
81 observed number of surviving follicles (and thus an estimate of ovulated eggs) over time. Although this

82 does not prove that the apparently complex process of follicle population dynamics is simple, the results
83 show that a relatively simple probability-dependent process is consistent with and could help us better
84 understand the process of follicle development in nature.

85 **Materials and Methods**

86 **Ethics statement**

87 “Wet lab” histomorphometric quantification of primordial follicles was performed according to the ap-
88 proved Yale IACUC Protocol #2013-11569.

89 **Markov chain modeling**

90 The term Markov chain, named after Russian mathematician Andrey Markov (1856-1922), refers to a
91 method for representing stochastic processes by dividing them into unique “states” in a chain. To be
92 modeled by a Markov chain, the states must be considered to behave independently of any past
93 behavior—a characteristic called “memorylessness.” The probability of moving on to any subsequent state
94 thus only depends on the present state. To model ovarian follicle development using a Markov approach,
95 we establish three states of follicle development (growth arrest, growth, and death; Figure 1) as meeting
96 this criterion. Individual follicles begin in the growth arrest state, and the state can either change or
97 stay the same according to random transition probabilities at each step moving forward in time (in the
98 simulation, days).

99 **Model structure**

100 A simplified example of the Markov matrix operations that we use to simulate follicle growth is seen
101 as follows in (1), where three growth-arrested follicles, A , B , and C are represented by vertical matrix
102 entries populated by one, three, and one “granulosa cell(s).”

$$\begin{array}{ccccccc}
 & A & B & C & & A & B & C & & A & B & C & & \\
 \text{Start} = & 1 & \mathbf{3} & \mathbf{1} & \rightarrow & \text{Step1} = & 1 & \mathbf{3} & \mathbf{1} & \rightarrow & \text{Step2} = & 1 & \mathbf{3} & \mathbf{1} & \dots & (1) \\
 & & & & & & 1 & \mathbf{6} & \mathbf{2} & & & 1 & \mathbf{6} & \mathbf{2} & & \\
 & & & & & & & & & & & 1 & \mathbf{10^*} & \mathbf{0^{**}} & &
 \end{array}$$

103

104 When the simulation begins, follicle states are calculated at each model step according to transition
 105 probabilities. In *Step1*, one example follicle (*A*) remains growth-arrested (e.g., its probability calculation
 106 results in the “Hold” state) and it maintains its number of pregranulosa cells. The other two follicles (*B*
 107 and *C*, indicated by bold, underlined numbers) growth activate in *Step1* (their probability calculations
 108 result in a state change from “Hold” to “Grow”). Existence within the “Grow” state means that follicles
 109 can either continue to grow or transition to the “Die” state. While growing, granulosa cell number
 110 approximately doubles each daily step. This (daily) doubling time reflects a granulosa cell mitotic index
 111 that is consistent with reported (22) and our own (Conca Dioguardi, Uslu, and Johnson, unpublished)
 112 data. In *Step2*, follicle *B* grows but is shown to contain less than double the number of granulosa cells
 113 in the previous step due to granulosa cell death (*; modeled as a Bernoulli random variable, details in
 114 $\bar{\text{OvSim}}$ R code, below; after (22) and Conca Dioguardi, Uslu, and Johnson, unpublished). Follicle *C* grew
 115 in *Step1*, but commits to atresia in *Step2* because its probability calculation resulted in the “Die” state,
 116 and its granulosa cell number is set to zero (**, see details in $\bar{\text{OvSim}}$ R code, below). These steps are
 117 represented in the Markov state transition diagram in Figure 1.

118 $\bar{\text{OvSim}}$ R code and model parameters

119 $\bar{\text{OvSim}}$ R code and accompanying documentation is available on GitHub ([https://github.com/](https://github.com/johnsonlab/OvSim)
 120 [johnsonlab/OvSim](https://github.com/johnsonlab/OvSim)) and has been released using the MIT License ([http://opensource.org/](http://opensource.org/licenses/MIT)
 121 [licenses/MIT](http://opensource.org/licenses/MIT); see Supporting Information). $\bar{\text{OvSim}}$ was designed using known biological parame-
 122 ters of ovarian follicles while allowing users to modify some of these parameters (Table 1). Once the
 123 script is activated, a numerical matrix is populated with randomly-generated values corresponding to the
 124 starting number of granulosa cells in individual simulated primordial follicles (e.g., one, two, or three
 125 pregranulosa cells per (23); see also “puberty” option below).

126 In $\bar{O}vSim$, the starting number of follicles in the ovary (NF), the number of days of time (ND) to run
127 the simulation, and the length of the ovulatory cycle ($cyclength$) can all be specified. We set the number
128 of mouse ovarian follicles to 3000, including 2250 primordial follicles (after (11) and (24)) for most of our
129 studies. Ovulatory cycle length for mice was set at 4, 4.5, or 5 days. As mentioned, we use a daily (e.g.,
130 24 hour) doubling time for granulosa cells and allow users to set the granulosa cell death rate fraction of
131 The script then continues to loop with “daily” probability calculations and operations upon each follicle
132 entry in the matrix. Simulations run for 420 days by default (14 months), corresponding approximately
133 the fertile lifespan of C57Bl/6 mice fed *ad libitum* (25).

134 Parameters related to follicle growth can be specified as follows. If used, the default *phold* variable is
135 the stationary probability that a primordial follicle stays growth arrested each day. Individual primordial
136 follicles either stay arrested and therefore maintain their cell number of 1, 2, or 3, or, growth activate.
137 Optionally, users can choose to simulate the action of the paracrine factor Anti-Müllerian Hormone
138 (AMH) upon follicle growth activation. AMH produced by growing follicles has been shown to inhibit
139 the growth-activation of primordial follicles (26; 27; 28). When the variable *phold* is set equal to the
140 string “*custom1*”, a non-stationary probability *phold.new* is used in place of *phold*. As the simulation
141 runs, *phold.new* is held at a user-specified value (in our example, 0.995) as follicle numbers decline. When
142 the number of immature follicles declines and reaches the threshold number entered into the variable
143 *threshold*, *phold.new* begins to decline at a user-specified rate per day. In either case, overcoming growth
144 arrest results in growth activation where an individual follicle represented in the matrix is released to a
145 state of exponential granulosa cell growth with a daily doubling time.

146 Granulosa cell number in growing follicles is controlled by the probability that individual cells within
147 a growing follicle survive (*pcelllive*). Our estimates using histological sections detect a background of
148 pyknotic granulosa cells between 15 and 20% within follicles thought to be intact. Thus (*pcelllive*) is
149 modeled as independent Bernoulli random variable within that range with 0.8 as the default value.

150 To control the fraction of follicles that commit to atresia, a conditional stationary probability, *cond.pdub*
151 is executed upon each matrix entry each day. As mentioned, the follicle’s matrix entry can double (minus
152 the cell death induced by *pcelllive*, above) with probability *cond.pdub*, Alternatively, the follicle can “die”
153 via atresia with the probability $1 - cond.pdub$. A follicle’s death is simulated by its matrix entry set to
154 zero.

155 The parameter *ejectnum* (50,000 by default) reflects the number of granulosa cells required for a follicle

156 to be categorized as a fully mature preovulatory follicle. Critically, the simulation as designed here does
157 not control the final stage(s) of follicle development that ensure that ovulation occurs on only one day
158 per cycle. For now, we are modeling growth patterns that can give rise to approximately ovulatory sized
159 follicles within an entire single ovulatory cycle (4 - 5 days in the mouse). Using (6) as a guide, we set
160 the threshold for survival to ovulation to 50,000 but experimented with thresholds as large as 500,000
161 granulosa cells.

162 We also added the ability to optionally begin the simulation placing the ovary in a peripubertal state,
163 where several hundred follicles have already reached the preantral stage of growth awaiting puberty. The
164 option “puberty,” when set to TRUE, populates a user-specified number of matrix entries (variable IGP
165 for initial growing pool) with granulosa cell numbers that range from newly growth-activated to the
166 estimated number of granulosa cells in peripubertal preantral follicles. The number of growing follicles
167 and the range of granulosa cells in this prepubertal growing pool can also be user defined.

168 Overall, it can be said that the model parameters were not formally estimated, but were instead
169 selected based on our domain expertise. The question was whether a simple model of follicle population
170 dynamics might recapitulate apparently complex patterns of follicle growth and survival seen *in vivo*.

171 **Mice and tissue collection**

172 C57BL/6 mice were handled and tissues were collected in accordance with an active protocol under the
173 auspices of the Yale IACUC. Fresh ovaries were removed and cleaned from the fat, rinsed in PBS and fixed
174 in Dietrich’s fixative (30% Ethanol (EtOH; v/v), 10% Formalin (v/v - using aqueous 37% Formaldehyde
175 solution), 2% Glacial Acetic Acid (v/v); filter prior to use) overnight. Ovaries were then transferred into
176 70% EtOH for storage at 4°C. Specimens were batched and embedded in paraffin. 5 μ m serial sections
177 were cut and placed onto glass slides (Fisher Superfrost/Plus Microscope slides-Pre-cleaned (#12-550-15).
178 Slides were warmed, dewaxed with Xylenes (3 times x 5 min.) and rehydrated through an increasing
179 alcohol series up to distilled water and then PBS. Slides were then stained in Weigert’s Iron Hematoxylin
180 for 10 min. followed by counterstaining in Methyl Blue (0.4 mg/ml in saturated aqueous Picric Acid) for
181 6 min. Finally, specimens were dehydrated and coverslipped in mounting media (Richard-Allan Scientific
182 Cytoseal-60 Low Viscosity (# 8310-16).

183 **Histomorphometric follicle counting of primordial follicles**

184 Primordial follicles were counted in every fifth serial section, with raw numbers multiplied by 5 as previ-
185 ously described (29; 30). A follicle was considered primordial if a single layer of flattened pre-granulosa
186 cells surrounded the oocyte.

187 **Results**

188 **Using $\bar{O}vSim$ to Simulate the Mouse Ovary**

189 To model the development of mouse ovarian follicles over a normal reproductive lifespan, the parameters
190 in the *follicle* function are initialized with “default” values shown in the following function declaration:

```
191 ovsim <- function(NF = 3000,  
192                 ND = 420,  
193                 IGP = 300,  
194                 phold = 0.995,  
195                 cond.pdub = 0.9,  
196                 pcelllive = 0.8,  
197                 cyclength = 4,  
198                 ejectnum = 50000,  
199                 puberty = TRUE,
```

200 Here, 3000 total follicles are present at the start, 2700 of which are primordial (1-3 granulosa cells),
201 and 300 are small growing follicles randomly modeled to have initiated growth in a prepubertal cohort.
202 The estrus cycle length is 4 days, and follicle survival to ovulatory size is “called” if granulosa cell number
203 reaches 50,000. A Markov chain state transition matrix for the stationary probabilities of our three states
204 (Hold, Grow, and Die) according to these settings is shown as follows in (2):

$$P = \begin{matrix} & \begin{matrix} Hold \\ Grow \\ Die \end{matrix} & \begin{bmatrix} 0.995 & 0.005 & 0 \\ 0 & 0.9 & 0.1 \\ 0 & 0 & 1 \end{bmatrix} \end{matrix} \quad (2)$$

205

206 Note that matrix entries that exceed 50,000 simulated granulosa cells are categorized as having survived

207 to ovulatory size, and that follicles that have committed to atresia must stay dead, and therefore their
208 probability of remaining in that state is 1. Figure 1 is a Markov state diagram that includes our default
209 user settings, including the optional setting where the action of AMH upon the probability of primordial
210 follicle growth activation is modeled.

211 Representative plots of $\bar{O}vSim$ output when an approximately 6-week-old mouse ovary is simulated
212 using default settings are shown in Figure 2. We have expressed model output to highlight how closely
213 $\bar{O}vSim$ resembles key biological ovarian outcomes when the mentioned settings were used. Users can alter
214 model settings or even the code itself in order to test hypotheses about follicle growth and survival.

215 Panel 2A shows the trend of decline of the primordial pool over time (range between 1st and 99th
216 percentiles) after execution of the simulation 1000 times, comparing the outcome when AMH action is not
217 simulated (gray hatched area, stationary *phold*) versus when AMH action is simulated using a threshold
218 of 100 growing follicles as the trigger for declining probability of growth arrest (black area, non-stationary
219 *phold.new*). Individual data points for actual counts of C57Bl/6 mouse follicles in histological sections
220 at 40 days, 3 months, 4 months, 6 months, 8 months, and one year (circles) are overlaid with simulated
221 data (circles). Panel 2B is a plot of the growth and death of individual follicles that die within the 420
222 days of simulated time (when AMH action is simulated). Granulosa cell number is represented by the
223 dashed lines, and the time (and follicle “size”) of death is indicated by the letter “D.” Last, Panel 2C is a
224 histogram plot of the distribution of follicles that survive to ovulatory size, grouped in 4 day increments
225 equivalent to the modeled estrus (e.g., ovulatory) cycle length (matches 2B, AMH action is simulated).
226 The number of eggs available for ovulation each cycle are therefore depicted. $\bar{O}vSim$ also provides CSV-
227 formatted data associated with these plots, useful for finer analyses of follicle size according to granulosa
228 cell number.

229 Preliminary application of $\bar{O}vSim$ to human follicle dynamics

230 Simulation parameters can also be set to conditions mimicking the human ovary, ovulatory cycle length,
231 and approximate reproductive lifespan. For a preliminary human simulation, we set an appropriate num-
232 ber of human primordial follicles at (50,000), the menstrual cycle length to 30 days, and simulated 35
233 years (unique variable Y, representing the span from approximate ages 15 to 50) of reproductive life. We
234 specified that approximately 1 in 10,000 primordial follicles growth activated per day (*phold*=0.9999) but
235 kept the follicle survival rate (*cond.pdub*) and the probability that individual granulosa cells (*pcelllive*)

236 survive the same as in the mouse simulations (0.88 and 0.75, respectively). For the larger human peri-
237 ovulatory follicle, we set the number of granulosa cells at 500,000. A summary of these parameters as
238 entered follows here.

```
239 human <- function(NF = 50000,  
240                   Y = 35,  
241                   ND = 365*Y,  
242                   IGP = 0,  
243                   phold = 0.9999,  
244                   cond.pdub = 0.88,  
245                   pcelllive = 0.75,  
246                   ejectnum = 500000,  
247                   cyclength = 30,  
248                   puberty = FALSE,  
249                   verbose = TRUE,  
250                   pdfname = NA)
```

251 Representative output from these settings showed follicles that die or survive to ovulatory size in
252 numbers that were reminiscent of human biological outcomes. The total number of follicles that survived
253 to periovulatory size (contain 500,000 granulosa cells) was 605, and the total number of atretic follicles
254 over time was 35403. This meant that 1.4 simulated follicles survived to periovulatory size per month over
255 the length of the simulation. Lacking any additional complexity beyond these parameters, the Markov
256 approach here came very close to the expected “one egg per cycle” output seen in most human natural
257 ovulatory cycles.

258 Discussion

259 The $\bar{O}vSim$ R function simulates ovarian follicle growth using user-definable parameters; when set ap-
260 propriately, simulations produce results that closely match numbers seen over reproductive life *in vivo*.
261 Follicles that growth activate, die, and reach ovulatory size match the numbers seen *in vivo* over time. Be-
262 cause the R code is freely available for evaluation, use, and alteration, any interested user can contribute
263 to what may eventually become a highly useful simulation of mammalian ovaries. In the meantime, this
264 approach has stimulated interesting discussions about mechanisms that might be at work controlling
265 follicle growth activation, growth, and survival

266 We emphasize that this is a complete but early-stage simulation using probabilities that account for
267 only a few of the known features of biological follicle development. In the mouse and human ovary,
268 paracrine signaling interactions between follicles impact the rate of follicle growth activation (26) and
269 perhaps follicle survival (31; 32). We and others can work to include finer details of follicle biology in
270 these types of simulations, including the inclusion of additional paracrine and endocrine signaling effects
271 known to affect follicle growth and survival. What is clear here, however, is that stationary probabilities
272 for growth activation and death in our simple model can result in biologically-relevant numbers of follicles
273 that survive to the ovulatory stage or die. The initial inclusion of a non-stationary threshold effect of
274 simulated AMH action resulted in output that matched actual mouse follicle numbers during aging even
275 more closely. As seen in actual mouse and human follicle counts, follicle growth activation accelerates as
276 the number of growing follicles is depleted. While follicle loss is of primary interest, it is also important
277 to consider how synchronization occurs *in vivo* such that those follicles that survive to reach ovulatory
278 size ovulate together on a single day.

279 The problem of synchronous follicle *availability* for ovulation can be solved by simple rules, but not the
280 more precise follicle *synchronization* such that all periovulatory follicles ovulate on a single day. Selection
281 for ovulation is solved by an additional layer of complexity, the hormonal ovulatory cycle. Ovulation
282 and the final stages of meiotic maturation occur after the LH surge on a single day of the ovulatory
283 cycle, favoring the production of mature eggs on the day of ovulation as well. The hormonal ovulatory
284 cycle can be considered as a “binning” or “winnowing” mechanism, acting upon and selecting follicles of
285 appropriate size to ensure that an appropriate number are ovulated only one day per cycle. The word
286 winnowing can imply the removal of undesirable elements, as in the potential removal of poorer quality
287 oocytes, but whether selection for high quality eggs does occur *in vivo* is unclear (33; 34; 35).

288 Ensuring that the number of eggs ovulated is tightly regulated in female mammals can be a matter
289 of life or death. Ovulating too few eggs could compromise the survival of a species if too few offspring
290 were produced over time. Ovulating too many eggs can also compromise the survival of a species.
291 Multiple gestation in humans is well known to be a significant risk factor for maternal and offspring loss
292 of life (36; 37; 38). Evolving mechanisms to ensure that the correct number of eggs are produced within
293 an organism’s overall reproductive strategy would therefore have been favored. It is striking that simple
294 regulatory mechanisms (e.g., constant growth activation and atresia rates) can solve much of the problem
295 of the periodic production of ‘safe’ numbers of eggs. Adding a level of ovulatory cyclicality to a future

296 version of $\bar{O}vSim$ will allow the control of ovulation timing to be simulated, and may provide clues about
297 the evolution of the ovulatory cycle itself.

298 $\bar{O}vSim$ trials show that just a few control parameters can give rise to patterns of asynchronous follicle
299 growth that appear complex. In this initial simulation model, the control parameters only include minimal
300 simulation of interaction(s) between follicles (AMH action). Follicle development within mammalian
301 ovaries may thus in some ways fit the criteria for the phenomenon called emergent behavior (39; 40).
302 Emergent behavior or emergent propert(ies) can appear when a number of simple entities (here, follicles)
303 operate in an environment and form more complex behaviors as a collective (the ovary). Another definition
304 of emergent behavior is any behavior of a system that is not a property of any of the components of that
305 system (40). The mouse (and human) ovary can be modeled as a “system of systems” where overall
306 organ behavior can arise from, but is not necessarily a property of, individual follicles.

307 Knowing that simple rules can control the number of follicles at different stages of development
308 and death in a fashion that mimics ovarian biology leads to hypotheses that can be tested in ‘wet lab’
309 experiments. We can test whether similar simple rules underlie ovarian function *in vivo*, and if so, what
310 mechanisms enforce those rules. For example, what mechanisms could control a fixed approximate 1%
311 growth activation rate and 10% overall atresia rate? How can seemingly equivalent primordial follicles
312 growth activate at such a constant rate without activating too quickly or slowly, ensuring that the total
313 duration of ovarian function is appropriate for the reproductive strategy of the female? How can the rate
314 of follicle atresia similarly remain so constant? Premature cessation of ovarian function could result if
315 the rate of either growth activation or atresia were increased (see (41) for a review). $\bar{O}vSim$ can also be
316 modified to model questions that are even more theoretical, such as the impact of ovotoxic agents (e.g.,
317 chemotherapeutic or radiological intervention(s)) upon the duration of ovarian function, or, the impact of
318 the additional of new follicles postnatally as suggested by studies that support postnatal oogenesis. The
319 example of the optional modeling of an anti-growth activation factor like AMH highlights the customizable
320 nature of $\bar{O}vSim$ and how users could evaluate the effects of any number of known mechanisms upon
321 simulation output.

322 The current prevailing consensus in the field is that oogenesis and folliculogenesis ceases before or
323 around birth in most mammals. However, since the first paper calling this into question (24), evidence
324 continues to build that postnatal follicle development can occur *via* the action of female germline stem
325 cells (FGSC) (42; 43; 44; 45; 46; 47; 48; 49; 50; 51; 52; 53). FGSC are currently being used as a source of

326 mitochondria (see (53) for a review) for delivery to oocyte cytoplasm in attempts to improve egg quality
327 and pregnancy rates in the clinic (54; 55). It is a relatively trivial matter to modify the $\bar{O}vSim$ *follicles*
328 function so that new follicles are added at a desired rate and the impact upon the trajectory of follicle
329 loss over time can be estimated. We will continue to develop flexible tools like $\bar{O}vSim$ to address these
330 exciting questions, and hope that other groups will modify the package and build on this approach.

331 **Supporting Information**

332 **$\bar{O}vSim$ Package Installation**

333 All package and supporting files are available on GitHub (<https://github.com/johnsonlab/OvSim>)
334 and has been released using the MIT License (<http://opensource.org/licenses/MIT>). $\bar{O}vSim$
335 can be installed in an R Environment by following the instructions in the file README.md. Alter-
336 natively, the single text file `ovsim.R` can be executed within R after optional alteration of individual
337 parameters.

338 **$\bar{O}vSim$ Package License**

339 $\bar{O}vSim$ is available under the conditions of The MIT License (MIT)

340 © 2015 Joshua Johnson and John W. Emerson

341 Permission is hereby granted, free of charge, to any person obtaining a copy of this software and associated
342 documentation files (the "Software"), to deal in the Software without restriction, including without
343 limitation the rights to use, copy, modify, merge, publish, distribute, sublicense, and/or sell copies of the
344 Software, and to permit persons to whom the Software is furnished to do so, subject to the following
345 conditions:

346 The above copyright notice and this permission notice shall be included in all copies or substantial
347 portions of the Software.

348 THE SOFTWARE IS PROVIDED "AS IS", WITHOUT WARRANTY OF ANY KIND, EXPRESS OR
349 IMPLIED, INCLUDING BUT NOT LIMITED TO THE WARRANTIES OF MERCHANTABILITY,
350 FITNESS FOR A PARTICULAR PURPOSE AND NONINFRINGEMENT. IN NO EVENT SHALL
351 THE AUTHORS OR COPYRIGHT HOLDERS BE LIABLE FOR ANY CLAIM, DAMAGES OR

352 OTHER LIABILITY, WHETHER IN AN ACTION OF CONTRACT, TORT OR OTHERWISE, ARIS-
353 ING FROM, OUT OF OR IN CONNECTION WITH THE SOFTWARE OR THE USE OR OTHER
354 DEALINGS IN THE SOFTWARE.

355 Acknowledgments

Drs. Giovanni Cottichio and Taiwo Togun are acknowledged for comments upon the manuscript prior to submission.

Funding

These studies were supported by a Milstein Medical Asian American Partnership Foundation Fellowship Award in Reproductive Medicine (X.C.) and The Albert McKern Fund for Perinatal Research (J.J.).

References

1. Reddy P, Liu L, Adhikari D, Jagarlamudi K, Rajareddy S, Shen Y, et al. Oocyte-specific deletion of Pten causes premature activation of the primordial follicle pool. *Science*. 2008 Feb;319(5863):611–613.
2. Adhikari D, Gorre N, Risal S, Zhao Z, Zhang H, Shen Y, et al. The safe use of a PTEN inhibitor for the activation of dormant mouse primordial follicles and generation of fertilizable eggs. *PLoS ONE*. 2012;7(6):e39034.
3. McLaughlin M, Kinnell HL, Anderson RA, Telfer EE. Inhibition of phosphatase and tensin homologue (PTEN) in human ovary in vitro results in increased activation of primordial follicles but compromises development of growing follicles. *Mol Hum Reprod*. 2014 Aug;20(8):736–744.
4. Cheng Y, Kim J, Li XX, Hsueh AJ. Promotion of ovarian follicle growth following mTOR activation: synergistic effects of AKT stimulators. *PLoS ONE*. 2015;10(2):e0117769.
5. Hsueh AJ, Kawamura K, Cheng Y, Fauser BC. Intraovarian control of early folliculogenesis. *Endocr Rev*. 2015 Feb;36(1):1–24.

6. Pedersen T, Peters H. Proposal for a classification of oocytes and follicles in the mouse ovary. *J Reprod Fertil.* 1968 Dec;17(3):555–557.
7. Anderson LD, Hirshfield AN. An overview of follicular development in the ovary: from embryo to the fertilized ovum in vitro. *Md Med J.* 1992 Jul;41(7):614–620.
8. Hirshfield AN. Development of follicles in the mammalian ovary. *Int Rev Cytol.* 1991;124:43–101.
9. Tilly JL, Kowalski KI, Johnson AL, Hsueh AJ. Involvement of apoptosis in ovarian follicular atresia and postovulatory regression. *Endocrinology.* 1991 Nov;129:2799–2801.
10. Inoue S, Watanabe H, Saito H, Hiroi M, Tonosaki A. Elimination of atretic follicles from the mouse ovary: a TEM and immunohistochemical study in mice. *J Anat.* 2000 Jan;196 (Pt 1):103–110.
11. Tilly JL. Ovarian follicle counts—not as simple as 1, 2, 3. *Reprod Biol Endocrinol.* 2003 Feb;1:11.
12. Kerr JB, Duckett R, Myers M, Britt KL, Mladenovska T, Findlay JK. Quantification of healthy follicles in the neonatal and adult mouse ovary: evidence for maintenance of primordial follicle supply. *Reproduction.* 2006 Jul;132(1):95–109.
13. Malki S, Tharp ME, Bortvin A. A Whole-Mount Approach for Accurate Quantitative and Spatial Assessment of Fetal Oocyte Dynamics in Mice. *Biol Reprod.* 2015 Nov;93(5):113.
14. Faire M, Skillern A, Arora R, Nguyen DH, Wang J, Chamberlain C, et al. Follicle dynamics and global organization in the intact mouse ovary. *Dev Biol.* 2015 Jul;403(1):69–79.
15. Skodras A, Marcelli G. Computer-generated ovaries to assist follicle counting experiments. *PLoS ONE.* 2015;10(3):e0120242.
16. Singh JA, Cameron C, Noorbaloochi S, Cullis T, Tucker M, Christensen R, et al. Risk of serious infection in biological treatment of patients with rheumatoid arthritis: a systematic review and meta-analysis. *Lancet.* 2015 Jul;386(9990):258–265.
17. Kirsch F. A systematic review of quality and cost-effectiveness derived from Markov models evaluating smoking cessation interventions in patients with chronic obstructive pulmonary disease. *Expert Rev Pharmacoecon Outcomes Res.* 2015 Apr;15(2):301–316.

18. Lampert A, Korngreen A. Markov modeling of ion channels: implications for understanding disease. *Prog Mol Biol Transl Sci*. 2014;123:1–21.
19. Jit M, Brisson M. Modelling the epidemiology of infectious diseases for decision analysis: a primer. *Pharmacoeconomics*. 2011 May;29(5):371–386.
20. Parker WH, Broder MS, Liu Z, Shoupe D, Farquhar C, Berek JS. Ovarian conservation at the time of hysterectomy for benign disease. *Clin Obstet Gynecol*. 2007 Jun;50(2):354–361.
21. R Development Core Team. R: A Language and Environment for Statistical Computing. Vienna, Austria; 2008. ISBN 3-900051-07-0. Available from: <http://www.R-project.org>.
22. Kadakia R, Arraztoa JA, Bondy C, Zhou J. Granulosa cell proliferation is impaired in the Igf1 null ovary. *Growth Horm IGF Res*. 2001 Aug;11(4):220–224.
23. Telfer E, Ansell JD, Taylor H, Gosden RG. The number of clonal precursors of the follicular epithelium in the mouse ovary. *J Reprod Fertil*. 1988 Sep;84(1):105–110.
24. Johnson J, Canning J, Kaneko T, Pru JK, Tilly JL. Germline stem cells and follicular renewal in the postnatal mammalian ovary. *Nature*. 2004 Mar;428(6979):145–150.
25. Selesniemi K, Lee HJ, Tilly JL. Moderate caloric restriction initiated in rodents during adulthood sustains function of the female reproductive axis into advanced chronological age. *Aging Cell*. 2008 Oct;7(5):622–629.
26. Durlinger AL, Kramer P, Karels B, de Jong FH, Uilenbroek JT, Grootegoed JA, et al. Control of primordial follicle recruitment by anti-Müllerian hormone in the mouse ovary. *Endocrinology*. 1999 Dec;140(12):5789–5796.
27. Durlinger AL, Gruijters MJ, Kramer P, Karels B, Kumar TR, Matzuk MM, et al. Anti-Müllerian hormone attenuates the effects of FSH on follicle development in the mouse ovary. *Endocrinology*. 2001 Nov;142(11):4891–4899.
28. Durlinger AL, Gruijters MJ, Kramer P, Karels B, Ingraham HA, Nachtigal MW, et al. Anti-Müllerian hormone inhibits initiation of primordial follicle growth in the mouse ovary. *Endocrinology*. 2002 Mar;143(3):1076–1084.

29. Tilly JL. Ovarian follicle counts—not as simple as 1, 2, 3. *Reprod Biol Endocrinol*. 2003 Feb;1:11.
30. Johnson J, Canning J, Kaneko T, Pru JK, Tilly JL. Germline stem cells and follicular renewal in the postnatal mammalian ovary. *Nature*. 2004 Mar;428(6979):145–150.
31. Moley KH, Schreiber JR. Ovarian follicular growth, ovulation and atresia. Endocrine, paracrine and autocrine regulation. *Adv Exp Med Biol*. 1995;377:103–119.
32. Webb R, Campbell BK. Development of the dominant follicle: mechanisms of selection and maintenance of oocyte quality. *Soc Reprod Fertil Suppl*. 2007;64:141–163.
33. Johnson J, Keefe DL. Ovarian aging: breaking up is hard to fix. *Sci Transl Med*. 2013 Feb;5(172):172fs5.
34. Titus S, Li F, Stobezki R, Akula K, Unsal E, Jeong K, et al. Impairment of BRCA1-related DNA double-strand break repair leads to ovarian aging in mice and humans. *Sci Transl Med*. 2013 Feb;5(172):172ra21.
35. Titus S, Stobezki R, Oktay K. Impaired DNA Repair as a Mechanism for Oocyte Aging: Is It Epigenetically Determined? *Semin Reprod Med*. 2015 Nov;.
36. Sciarra JJ, Keith LG. Multiple pregnancy: an international perspective. *Acta Genet Med Gemellol (Roma)*. 1990;39(3):353–360.
37. Ananth CV, Joseph Ks Ks, Smulian JC. Trends in twin neonatal mortality rates in the United States, 1989 through 1999: influence of birth registration and obstetric intervention. *Am J Obstet Gynecol*. 2004 May;190(5):1313–1321.
38. Uthman OA, Uthman MB, Yahaya I. A population-based study of effect of multiple birth on infant mortality in Nigeria. *BMC Pregnancy Childbirth*. 2008;8:41.
39. Saunders P, Skar P. Archetypes, complexes and self-organization. *J Anal Psychol*. 2001 Apr;46(2):305–323.
40. Cohen IR, Harel D. Explaining a complex living system: dynamics, multi-scaling and emergence. *J R Soc Interface*. 2007 Apr;4(13):175–182.

41. Silber S. Unifying theory of adult resting follicle recruitment and fetal oocyte arrest. *Reprod Biomed Online*. 2015 Oct;31(4):472–475.
42. Zou K, Yuan Z, Yang Z, Luo H, Sun K, Zhou L, et al. Production of offspring from a germline stem cell line derived from neonatal ovaries. *Nat Cell Biol*. 2009 May;11(5):631–636.
43. Pacchiarotti J, Maki C, Ramos T, Marh J, Howerton K, Wong J, et al. Differentiation potential of germ line stem cells derived from the postnatal mouse ovary. *Differentiation*. 2010 Mar;79(3):159–170.
44. Zhang Y, Yang Z, Yang Y, Wang S, Shi L, Xie W, et al. Production of transgenic mice by random recombination of targeted genes in female germline stem cells. *J Mol Cell Biol*. 2011 Apr;3(2):132–141.
45. Zou K, Hou L, Sun K, Xie W, Wu J. Improved efficiency of female germline stem cell purification using fragilis-based magnetic bead sorting. *Stem Cells Dev*. 2011 Dec;20(12):2197–2204.
46. White YA, Woods DC, Takai Y, Ishihara O, Seki H, Tilly JL. Oocyte formation by mitotically active germ cells purified from ovaries of reproductive-age women. *Nat Med*. 2012 Mar;18(3):413–421.
47. Woods DC, Tilly JL. Isolation, characterization and propagation of mitotically active germ cells from adult mouse and human ovaries. *Nat Protoc*. 2013 May;8(5):966–988.
48. Imudia AN, Wang N, Tanaka Y, White YA, Woods DC, Tilly JL. Comparative gene expression profiling of adult mouse ovary-derived oogonial stem cells supports a distinct cellular identity. *Fertil Steril*. 2013 Nov;100(5):1451–1458.
49. Park ES, Woods DC, Tilly JL. Bone morphogenetic protein 4 promotes mammalian oogonial stem cell differentiation via Smad1/5/8 signaling. *Fertil Steril*. 2013 Nov;100(5):1468–1475.
50. Zhou L, Wang L, Kang JX, Xie W, Li X, Wu C, et al. Production of fat-1 transgenic rats using a post-natal female germline stem cell line. *Mol Hum Reprod*. 2014 Mar;20(3):271–281.
51. Xie W, Wang H, Wu J. Similar morphological and molecular signatures shared by female and male germline stem cells. *Sci Rep*. 2014;4:5580.

52. Khosravi-Farsani S, Amidi F, Habibi Roudkenar M, Sobhani A. Isolation and enrichment of mouse female germ line stem cells. *Cell J.* 2015;16(4):406–415.
53. Woods DC, Tilly JL. Autologous Germline Mitochondrial Energy Transfer (AUGMENT) in Human Assisted Reproduction. *Semin Reprod Med.* 2015 Nov;.
54. Oktay K, Baltaci V, Sonmezer M, Turan V, Unsal E, Baltaci A, et al. Oogonial Precursor Cell-Derived Autologous Mitochondria Injection to Improve Outcomes in Women With Multiple IVF Failures Due to Low Oocyte Quality: A Clinical Translation. *Reprod Sci.* 2015 Dec;22(12):1612–1617.
55. Fakhri MH, El Shmoury M, Szeptycki J, de la Cruz D, Lux C, Verjee S, et al. The AUGMENTSM Treatment: Physician Reported Outcomes of the Initial Global Patient Experience. *JFIV Reprod Med Genet.* 2015;3:154.

Figure Legends

Figure 1. Markov state transition diagram of mouse ovarian follicle development. This flow chart shows the simplified logic of follicle development. From left to right, the first decision for an individual primordial follicle (numerical matrix entry of 1, 2, or 3 granulosa cells) is whether to remain arrested (“Hold”) or to growth activate (“Grow”). This can be simulated as stationary probability *phold* for the duration of the simulation (above dashed line, 0.995), or, as a non-stationary probability *phold.new* where the likelihood of remaining growth arrested gradually decreases from 0.995 to 0.990 as the number of growth-arrested follicles reaches a threshold. Growth activation introduces a daily doubling of granulosa cell number. A follicle may then either grow or die daily, with a correction factor of cell death applied to granulosa cell number. If a follicle reaches a threshold number of granulosa cells, it is categorized as an ovulatory follicle.

Figure 2. Example $\bar{O}vSim$ mouse ovary output. Default plots produced after an $\bar{O}vSim$ run with “puberty” option set to TRUE, and comparing output for stationary probability of follicle growth activation versus when AMH action is (optionally) simulated. X-axes represent total simulated time in days; pubertal animals would be approximately 50 days old at the start of the simulation. The trajectory of decline of the primordial follicle pool for 1000 $\bar{O}vSim$ runs is plotted as shown in panel **A** where the shaded areas span the first and 99th percentiles of run output when AMH is not simulated (stationary *phold* probability, light gray area) and when AMH is simulated (non-stationary *phold.new*, dark grey area). Circles are actual data from follicle counts of C57Bl/6 mice at 40 days, 3 months, 4 months, 6 months, 8 months, and one year of age ($n = 4$ ovaries, each from a different animal). In **B**, the growth history of individual follicles that die *via* atresia in a single run (matching run in A when AMH is simulated) is shown by plotting the number of granulosa cells (dashed line) over time, ending with follicle death denoted by the letter “D.” **C** shows the number of follicles that survive to ovulatory size cutoff (50,000 granulosa cells) each ovulatory cycle (here, 4 days), and dashed vertical lines mark months of time within a single simulation run (*phold.new*, AMH action is simulated).

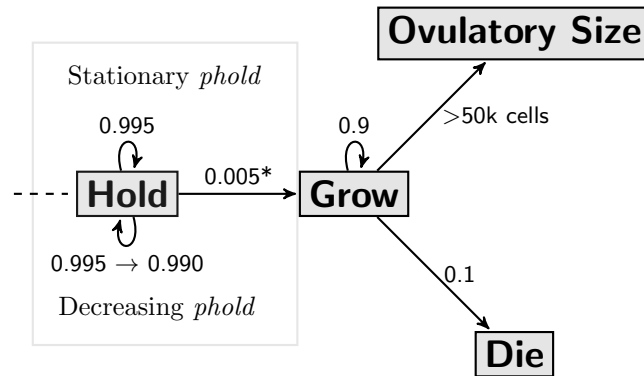


Figure 1. Mouse Ovarian Follicle Markov State Transition Diagram.

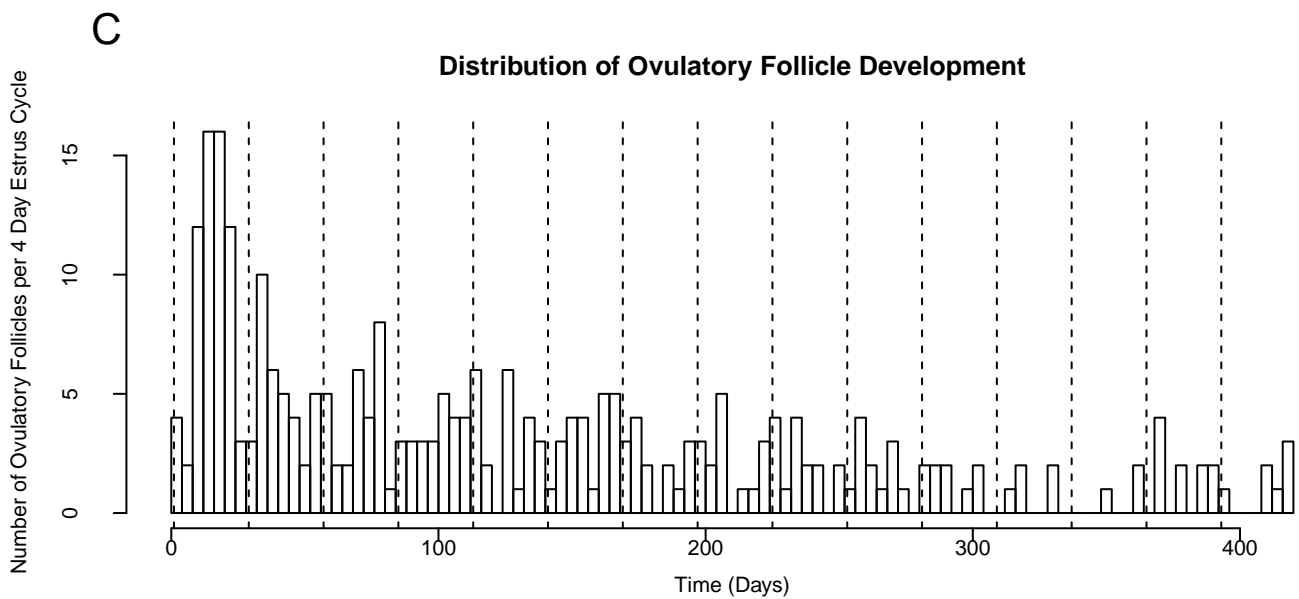
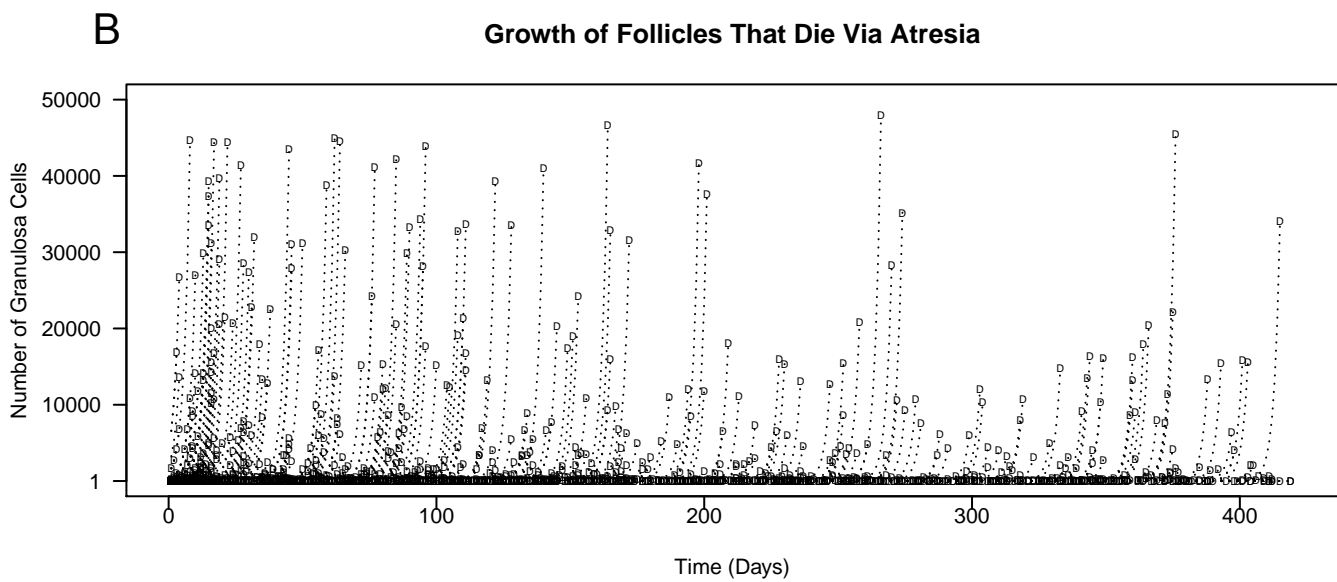
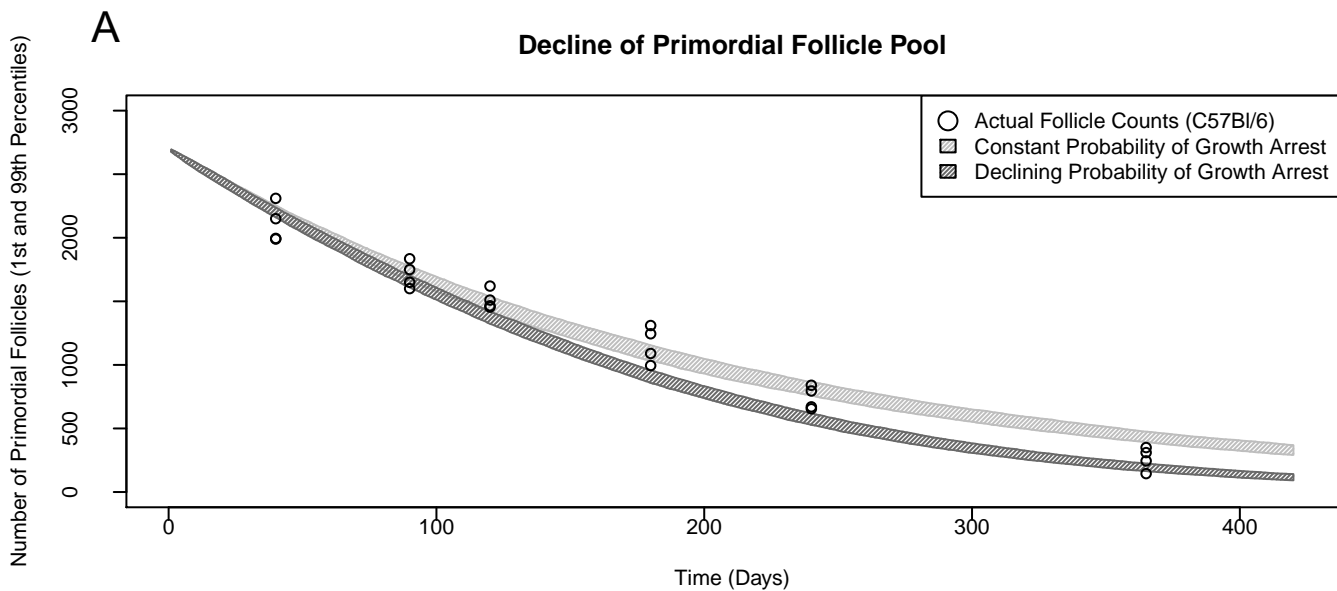


Figure 2. Example OvSim mouse ovary output.